

# Toughness Assessment of Elastomeric Polypropylene (ELPP) by the Essential Work of the Fracture Method

D. E. MOUZAKIS,<sup>1</sup> M. GAHLEITNER,<sup>2</sup> J. KARGER-KOCSIS<sup>1</sup>

<sup>1</sup>Institute for Composite Materials Ltd, University of Kaiserslautern, P.O. Box 3049, D-67653 Kaiserslautern, Germany

<sup>2</sup>PCD Polymere GmbH, P.O. Box 675, A-4021 Linz, Austria

Received 4 December 1997; accepted 6 January 1998

**ABSTRACT:** The essential work of the fracture (EWF) method was employed to determine the fracture performance of thermoplastic polypropylene (PP) elastomers. Three types of elastomeric polypropylene (ELPP) of homo- and copolymer nature based on different catalysts were involved in this study. Tests were carried out in both I and III fracture modes to check the applicability of the EWF approach for such elastomers. It was found that the trouser tearing test (mode III) overestimates both the specific essential ( $w_e$ ) and plastic work ( $w_p$ ) terms when the tearing resistance of the ELPP is higher than the resistance to tensile loading. With decreasing crystallinity (i.e., by decreasing length of the stereoregular chain segments of the block copolymers or increased content of comonomer)  $w_e$  increased, whereas in respect to  $w_p$ , an opposite tendency was found. This was interpreted by possible changes in the thermoreversible network structure of the ELPP in which crystalline domains act as network knot points in the amorphous PP matrix. © 1998 John Wiley & Sons, Inc. *J Appl Polym Sci* 70: 873–881, 1998

**Key words:** essential work of fracture; fracture mechanics; trouser tearing test; elastomeric polypropylene (ELPP); block copolymer; mode I; mode III; atactic–isotactic sequence

## INTRODUCTION

Thermoplastic elastomers of various types are gaining acceptance in recent years in different application fields. This is due to their good mechanical performance (including resilience) and easy recyclability. Although their set (compression and tensile) properties are below the crosslinked rubbers, thermoplastic elastomers are penetrating in the traditional rubber markets. This trend is supported by proper design guidelines, taking into consideration the weak sites of thermoplastic elastomers. Block copolymers form the major group of thermoplastic elas-

tomers. Here, the thermoreversible physical network structure is given either by phase separation (amorphous systems) or by crystallization (semicrystalline types).

Elastomeric polypropylene<sup>1–5</sup> (ELPP) represents a new member of the family of crystalline thermoplastic elastomers produced by metallocene synthesis. The significant commercial interest for ELPP is traced by the potential to replace soft (plasticized) PVC or even high-priced thermoplastic elastomers (TPEs). Although some details on microstructure are still open, ELPP grades are considered for commercialization. ELPP exhibits high elastic recovery and ultimate elongation ( $\sim 1000\%$ ) and acceptable tensile strength (between 2 and 30 MPa). The application regime of ELPP is confined between the melting ( $T_m \sim 150^\circ\text{C}$ ) and glass transition temperature ( $T_g$

Correspondence to: J. Karger-Kocsis.

*Journal of Applied Polymer Science*, Vol. 70, 873–881 (1998)

© 1998 John Wiley & Sons, Inc.

CCC 0021-8995/98/050873-09

**Table I Basic Thermal and Mechanical Properties of the ELPP According to Standard Characterization Techniques ( $T_m$  and  $T_g$  from DSC acc. to ISO 3146, Tensile Data from Tensile Test acc. to ISO 527 at +23°C, Tensile Impact acc. to ISO 8256 at +23°C)**

Material	$T_m$ (°C)	$T_g$ (°C)	$E$ -modulus (MPa)	Ultimate Stress, $\sigma_B$ (MPa)	Ultimate Strain, $\epsilon_B$ (%)	Tensile Impact Energy (kJ/m <sup>2</sup> )
ELPP-A	158	+4	290	~ 10.0	750	280
ELPP-B	154	-5	25	2.4	1000	300
ELPP-C	140	-10	18	1.0	1000	290

~ -5°C). However, this envelope can be broadened by copolymerization or blending with other polymers having lower  $T_g$  or higher melting temperatures. The discovery of organometallic catalysts<sup>4,5</sup> allowing the production of this specific type of ELPP built up from atactic (amorphous) and isotactic (crystalline) PP segments, triggered further R&D activities to tailor its thermal and mechanical properties.

The essential work of fracture (EWF) is a valuable method for estimation of the fracture toughness of ductile polymers. Surprisingly, this approach is less applied to study the fracture behavior of thermoplastic elastomers. Our efforts were, therefore, focussed on investigating the fracture response of ELPP by means of the EWF theory, and to elucidate whether or not the use of this approach is limited for thermoplastic elastomers.<sup>6</sup>

## EXPERIMENTAL

### Materials

Three different types of ELPP, delivered in the form of compression molded quadratic (225 × 225 mm<sup>2</sup>) plates of about 2 mm thickness, were involved in this study. All of them had the same melt flow index (MFI = 0.5 g/min at 230°C and 2.16 kg load). All ELPP grades are of block copolymer type; they were produced by catalytic polymerization in liquid/bulk mode. The basic difference between them lies in the nature of the catalyst: type A was based on a conventional Ziegler-Natta-type catalyst without an electron donor, while types B and C were based on a tetra-naphyl-zirconium-type catalyst,<sup>4</sup> and in the fact that types A and B were homopolymers, which contain atactic and isotactic PP segments solely, whereas C was an ethylene/propylene random copolymer. All of these ELPP grades exhibit

thermoplastic elastomeric behavior. Data on the basic thermal and mechanical properties of the ELPP investigated are given in Table I. On a molecular level, type A is characterized by a stereoregularity (*mmmm*-pentad content<sup>6</sup>) of approx. 60%, while types B and C have a stereoregularity of 40%, and type C additionally contains approx. 3 mol % of ethylene. The systems further on will be referred to as: ELPP-A, -B, and -C, respectively.

### Thermal Analysis

The thermal and thermomechanical properties of ELPP were studied by differential scanning calorimetry (DSC) and dynamic-mechanical thermoanalysis (DMTA). A Mettler<sup>®</sup> DSC 30 (Mettler-Toledo, Gräfelswald, Switzerland) was employed to record the DSC traces in the range of -100 . . . +200°C, both in heating and cooling regimes. For the heating and cooling, a rate of 10°C/min was selected. DMTA tests were conducted on an Eplexor<sup>®</sup> 150 N (Gabo Qualimeter, Ahlden, Germany). Viscoelastic material parameters such as mechanical loss factor and complex tensile Young's modulus ( $\tan \delta$  and  $E^*$ , respectively) were measured in tensile loading over a broad temperature range (-100 . . . +180°C). Heating of the specimens occurred at 1°C/min. Specimens with a dimension of 70 × 10 mm (length × width) were stamped from the plates and subjected to sinusoidal loading ( $3 \pm 0.1$  N) superimposed to a static preload ( $6 \pm 0.2$  N) at a frequency of 10 Hz.

### Mechanical Tests

For the static loading of the deeply double edge-notched (DDEN-T, mode I) and trouser tearing (mode III) specimens, a Zwick 1248 type (Ulm, Germany) universal testing machine was used. The testing conditions in both cases were: deformation rate  $v = 1$  mm/min and temperature  $T = 23^\circ\text{C}$ .

The essential work of the fracture (EWF) approach was adopted, which works well for the fracture characterization of toughened polymers or polymers exhibiting gross yielding during fracture.<sup>6,8-10</sup> However, the limits of the application of the EWF are not yet fully defined. There has been even some dispute<sup>11</sup> about the validity of the method in respect to viscoelastic effects (which are inherent properties of polymers), but there is practically no alternative to study the fracture of such polymers.

According to the EWF theory,<sup>6,8-10</sup> credited to Broberg,<sup>12</sup> the total energy required to fracture a notched specimen can be distinguished in two components: the essential work of the fracture ( $W_e$ ), and the nonessential or plastic work of the fracture ( $W_p$ ), respectively. The first term is related to the energy that is demanded during fracture of the polymer in the crack process plane and thus generating new surfaces.  $W_p$  is the actual energy dissipated in the outer plastic region of the crack zone where various types of deformations may take place. Therefore,  $W_e$  is surface related, whereas  $W_p$  is a function of the deformed plastic zone volume. The latter depends on the deformation mechanisms (affecting the shape of the plastic zone), which is strongly influenced by testing conditions.<sup>13</sup> The total fracture energy,  $W_f$ , being the integral of force over displacement as measured during the tests, can thus be expressed by:

$$W_f = W_e + W_p \quad (1)$$

Considering the aforementioned surface ( $lt$ ) and volume-dependence ( $l^2t$ ) of the constituent terms, eq. (1) can be rewritten by the specific terms of essential and nonessential work of the fracture:

$$W_f = w_e \cdot lt + \beta w_p \cdot l^2t \quad (2)$$

$$w_f = \frac{W_f}{lt} = w_e + \beta w_p l \quad (3)$$

where  $l$  is the ligament length,  $t$  is the specimen thickness, and  $\beta$  is a shape factor related to the form of the plastic zone. Obviously,  $w_e$  can be estimated from the interception of the linear regression of the plot of  $w_f$  vs.  $l$ , with the  $w_f$  axis. On the other hand,  $w_p$  can be calculated from the slope of the linear regression  $w_f$  vs.  $l$ , provided that the shape of the plastic zone is well defined. This prerequisite is actually very important, be-

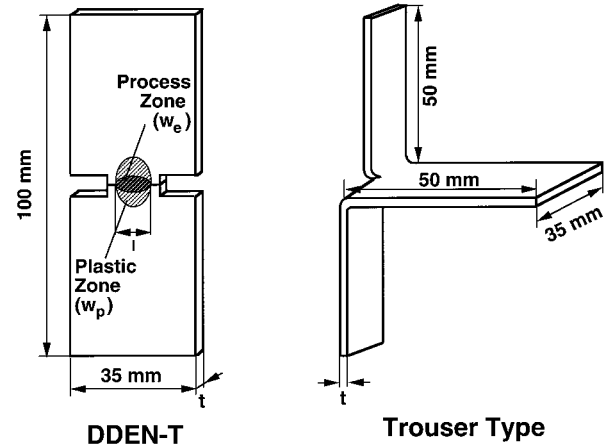


**Figure 1.** Size and loading mode of the specimens used.

cause in the absence of it, an exact determination of the plastic work is impossible.

The EWF parameters can be easily determined by using DDENT specimens.<sup>14</sup> Another interesting approach is the one that correlates polymer tear strength with  $w_e$  and  $w_p$ ; hence, both these can be also deduced from the so-called trouser tearing tests (cf. Fig. 1) already successfully applied for thin polymer films.<sup>15,16</sup> A major difference between these tests relies on the loading mode: mode I for DDENT, and mode III for trousers tear. During trouser tearing of the specimen, the force usually rises until reaching an equilibrium level—where steady tearing takes place—and falls finally, marking the ultimate failure. The force equilibrium value can be related with the specific essential and nonessential work of the fracture through:

$$w_e = \frac{F}{t^2} = 2w_p t \quad (4)$$

An important prerequisite of the test is that during tearing, legs of the torn specimen should not elongate and dissipate energy. It should be emphasized here that the  $w_e$  and  $w_p$  values derived from the aforementioned mode I and mode III tests may differ considerably from one another. This is linked to the deformability of the local microstructure.<sup>16</sup>

## RESULTS AND DISCUSSION

### Thermal Analysis

The DSC traces taken during heating of the sample (cf. Fig. 2) show a  $T_g$  step at  $T \sim 10^\circ\text{C}$ , followed

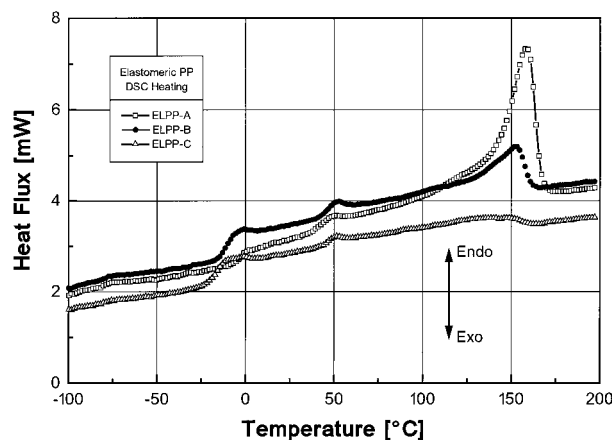


**Figure 2.** Comparison of the DSC heating traces for the ELPP samples.

by a small endotherm at  $T \sim 50^\circ\text{C}$  and a more pronounced endothermic peak at  $T \sim 155^\circ\text{C}$ . The latter is definitely due to the melting of the crystallized phase formed by cocrystallization of the stereoregular molecular sequences. The shift toward lower melting temperatures, when compared to the usual isotactic PP ( $T_m \sim 165^\circ\text{C}$ ), can be explained by the presence of less perfect crystals and other crystalline modifications than the  $\gamma$ -form (e.g., the  $\gamma$ -form). The melting peak is far less pronounced for ELPP-C where the crystallization is additionally hampered by the chain irregularities caused by the insertion of ethylene. As expected, a large undercooling can be recognized when comparing the melting and crystallization ( $T_c$ ) peaks registered in heating and cooling, respectively (cf. Figs. 2 and 3). It becomes obvious that, with increasing amount of the ste-

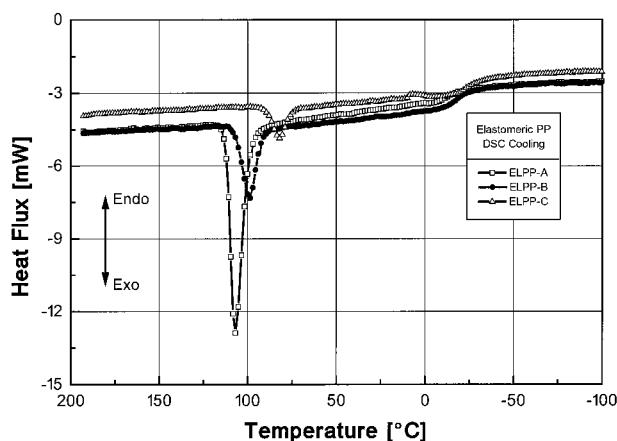


**Figure 3.** Comparison of the DSC cooling traces for the ELPP samples.

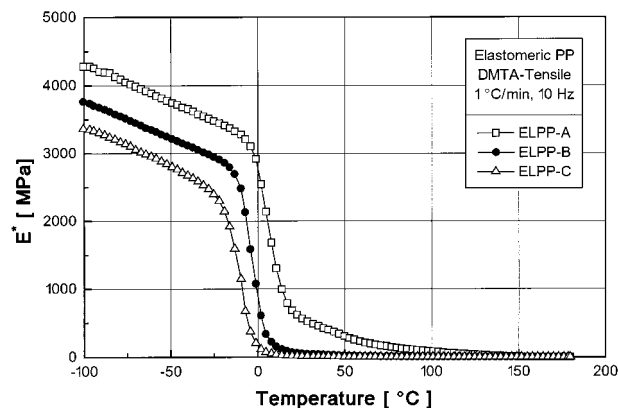


**Figure 4.** DMTA spectra ( $E^*$  vs.  $T$ ) for the ELPP samples.

reoregular (i.e., isotactic) PP segments, the undercooling (defined as the difference between  $T_m$  and  $T_c$ ) decreases. The undercooling is thus smallest for ELPP-A and largest for ELPP-C. The  $T_g$  step in Figure 3, however, at a slightly lower temperature ( $T_g \sim -15^\circ\text{C}$ ) than during heating, can well be resolved. For this shift kinetic effects are responsible. It is rather puzzling that no crystallization pendant of the melting peak at  $T \sim 50^\circ\text{C}$  (cf. Fig. 2) was found during cooling (cf. Fig. 3). The most possible reason for this is that the formation of crystalline aggregates, which melt at this  $T$  range, occurs by physical aging beyond  $T_g$ . Therefore, this melting peak can be found only on specimens stored for a longer time at or above ambient temperatures. This suggestion is supported by the fact, that in the second melting of the freshly cooled sample, the melting range at  $T \sim 50^\circ\text{C}$  was lacking.

The DMTA spectra ( $E^*-T$ ) in Figure 4 clearly

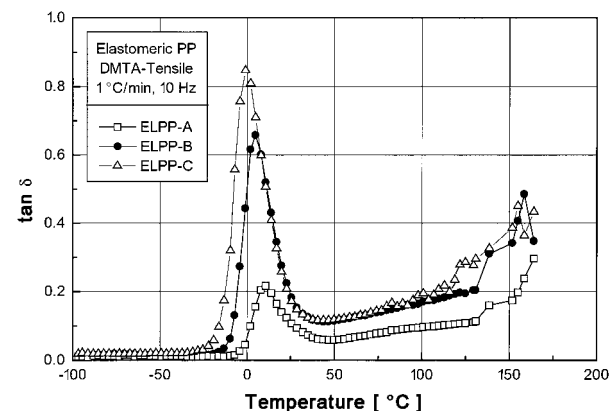


**Figure 5** DMTA spectra ( $\tan\delta$  vs.  $T$ ) for the ELPP systems.

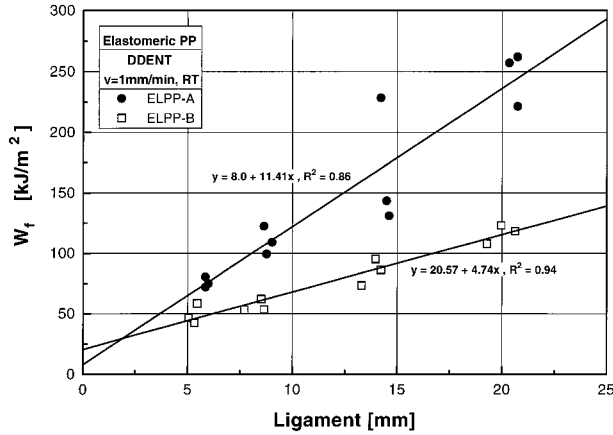


**Figure 6.** Specific work of fracture ( $w_f$ ) data vs. ligament plots and corresponding linear regressions for the ELPP-A and -B samples.

demonstrate that the stiffness of the ELPP is increased with increasing the amount of the isotactic segments of the block copolymers. The molecular buildup affects the  $T_g$ : based on the inflexion point of the  $E^*-T$  curves, the  $T_g$  of ELPP-A, -B, and -C are as follows: 8, -2, and 8°C, respectively. These data conform with the DSC results as discussed above. The shift in the  $T_g$  is also well displayed in the  $\tan \delta-T$  curves (Fig. 5). One can recognize that increasing amounts of the crystallizable segments of the block copolymers result in a decrease of the mechanical damping, as expected. The small  $\tan \delta$  peak at  $T \sim 130^\circ\text{C}$  for ELPP-C is likely to be an effect of strain-induced crystallization.

### Essential Work of Fracture

As mentioned before, the applicability of the EWF method depends on whether or not a clear distinction can be made between the process and plastic zones. ELPP-C was disregarded during the tests

on DDEN-T specimens because in that case this prerequisite was not met. Furthermore, a significant crack-tip blunting occurred that was not followed by steady crack propagation. On the other hand, the mode III tearing test worked well for this ELPP-C, allowing us to derive both  $w_e$  and  $w_p$  parameters. Figure 6 shows the data reduction for the DDEN-T specimens cut from ELPP-A and -B, respectively. Figure 6 makes clear that, with decreasing crystallinity (i.e., decreasing the amount of the crystallizable stereoregular sequence in the block copolymer),  $w_e$  increases, whereas the opposite trend can be recognized in respect to the slope of the  $w_f$  vs.  $l$  curves. To estimate the shape parameter  $\beta$  [see eq. (3)], the height of the plastic zone was plotted against the ligament. Supposing an elliptical shape, for which

$$\beta = \frac{\pi h}{4l} = 0.785 \frac{h}{l}$$

is valid,<sup>14</sup> the parameter could be computed from the slope of the regression curves. It should be noted here, that the development of the plastic zone in the DDEN-T specimens was accompanied with some change in the opacity that could be observed using transmitted light. The results on  $w_e$  and  $w_p$  determined in mode I and III type tests, respectively, are listed in Table II.

Comparing the  $w_e$  data, a large difference between the two loading modes was found. The elongation of the trouser specimen legs is responsible for the unrealistic high  $w_e$  values under mode III. One can thus conclude that the trouser test is not straightforward when the tearing resistance of the polymer is higher or commensurable with that of the tensile loading. The tear strength of the ELPP-C specimens is considerably lower than ELPP-A and -B; therefore, the  $w_e$  value is likely to be correct. Recall that the mode III  $w_e$  value of

**Table II** Essential and Plastic Work Terms for the ELPP Systems Studied in Mode I and III Type Loading

Material	$\beta$ (-)	$w_e$ [kJ/m <sup>2</sup> ]		$w_p$ [MJ/m <sup>3</sup> ]	
		Mode I	Mode III	Mode I	Mode III
ELPP-A	0.21	8.0	(294.0)	53.8	(73.7)
ELPP-B	0.50	20.6	(73.4)	9.4	(18.7)
ELPP-C	—	—	30.3	—	9.8

Tear test results are based on five parallel specimens; the unrealistic data due to deformation of the trouser leg are marked by brackets.



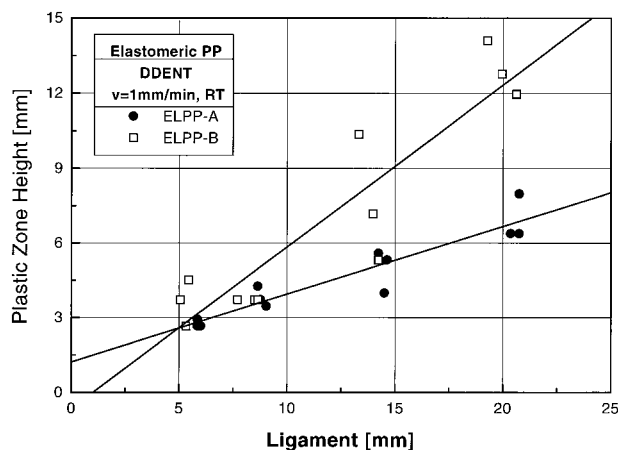


**Figure 7.** Plastic zone height vs. ligament plots and corresponding linear regressions for DDENT specimens, of ELPP-A and -B, respectively.

ELPP-C fits into the structure-related expected ranking of the ELPP types.

The nonessential or plastic work of the ELPP systems decreases with decreasing the amount of the crystallizable (stereoregular) sequence of the block copolymers. This finding can be better explained by accounting for the network structure of the ELPP. The knot points of the thermoreversible (physical) network structure are given by crystallites produced via cocrystallization of stereoregular segments of several polymeric chains. The size of such aggregates, and thus the “tightness” of the network (controlling the strength of the ELPP) increase with longer stereoregular chain sequences. The amorphous, “soft” segments act as tie molecules between the knot points and form the matrix. The probability of additional

entanglement network formation becomes more likely with increasing length of the noncrystallizable (atactic) segments of the chains. One can thus suppose that the change from ELPP-A toward ELPP-C is associated with the formation of an entanglement network. The latter can be considered as a very broad meshed network that may coexist with that composed of crystallites. It is obvious that the stress transfer and redistribution via molecular entanglement is completely different from a network in which the knot points are formed by crystalline domains. The molecular damage of the latter is more localized (that is the reason why the formation of plastic zone was observed for ELPP-A and -B under mode I deformation) than in the case of a molecular entanglement. It can be summarized that the plastic work is likely linked to the presence of the network structure formed by crystallites, and thus should depend on its characteristics (e.g., domain size, breaking up, and rearrangement of the crystallites due to mechanical loading). This is the reason why the plastic work is highest for ELPP-A. On the other hand, the essential work of the fracture seems to depend on the characteristics (e.g., mean length and density) of the tie molecules connecting either the crystalline domains or the entangling points. This is the possible rationale why  $w_e$  is increasing according to the ranking ELPP-A < -B < -C. Recent studies performed on amorphous copolyesters corroborated the assumption about the role of the entanglement network.<sup>13,17</sup> Unfortunately, the above proposed scenario is still speculative. Further investigations are needed (e.g., wide- and small-angle X-ray scattering during deformation) to verify it.

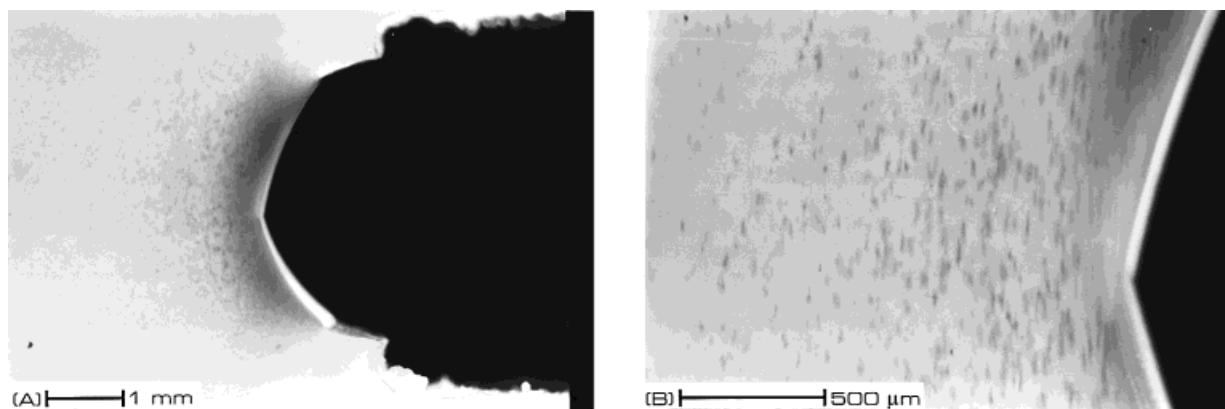


**Figure 8.** *In situ* light microscopy photographs from the crack tip of a DDEN-T specimen of ELPP-A.

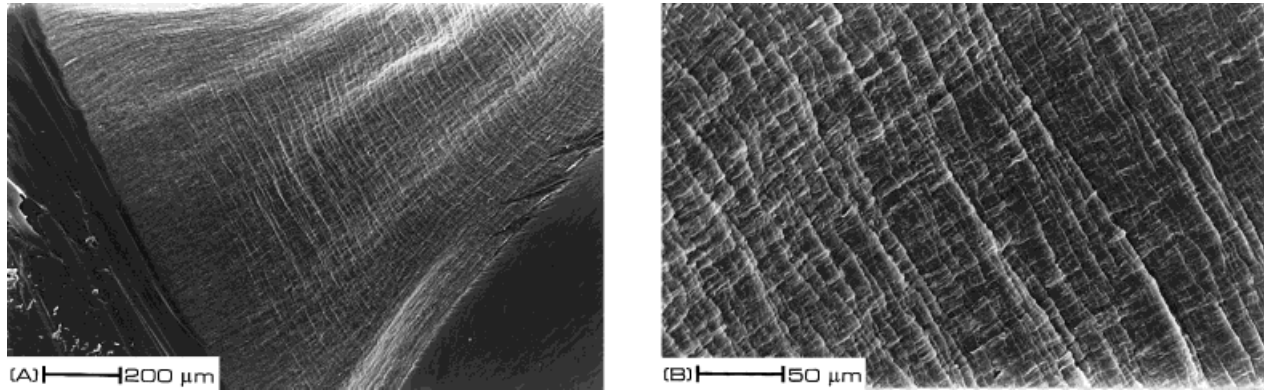


**Figure 9.** SEM pictures taken from the fracture surface of a DDEN-T specimen of ELPP-A.

### Fractography

*In situ* light microscopic frames taken during static fracture of DDEN-T specimens revealed interesting facts, especially about the ELPP-A type of elastomer. In Figure 8, pictures taken from the surface of the plastic zone of a DDEN-T specimen of ELPP-A are shown. Some kind of stress whitening (darker area) is visible in Figure 8(a). At higher magnification this area seems to consist of some kind of elliptical microvoids oriented parallel to the load axis. Careful observation using both transmitted and reflected light microscopy proved that these voids formed only in the bulk material and not on the surface of the plastic zone. Cavities are known to be initiated in particle-toughened polymers, on the boundaries between inclusions and matrix,<sup>18,19</sup> a mechanism also referred to as debonding. Local stress concentrations leading to debonding, and consequently cavitation, may be generated across the inter-

phase between crystalline and amorphous areas within the physical network structure of semi-crystalline thermoplastic elastomers. No cavitation or any other stress-whitening effect was observed, however, for the B and C types of ELPP. This finding seems to be in concert with our previous interpretation on the microstructural dependence of  $w_p$ .

Fracture surface topography of the DDEN-T specimens of ELPP-A and ELPP-B was investigated by scanning electron microscopy (SEM) as well. A rather smooth fracture area is seen in Figure 9(a) for ELPP-A, clearly necked under the influence of the tensile load. A careful examination under higher magnification reveals striation lines just after the crack initiation [cf. Fig. 9(b)]. In the formation of these striation bands the contraction of the elastomeric matrix in the stage of steady crack propagation should be involved. On the other hand, fractography of ELPP-B resulted

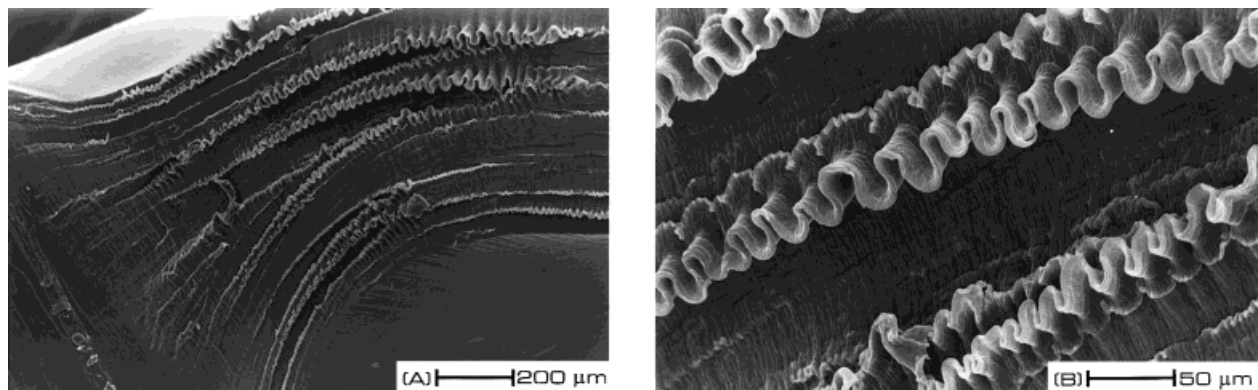


**Figure 10.** SEM pictures taken from the fracture surface of a DDEN-T specimen of ELPP-B.

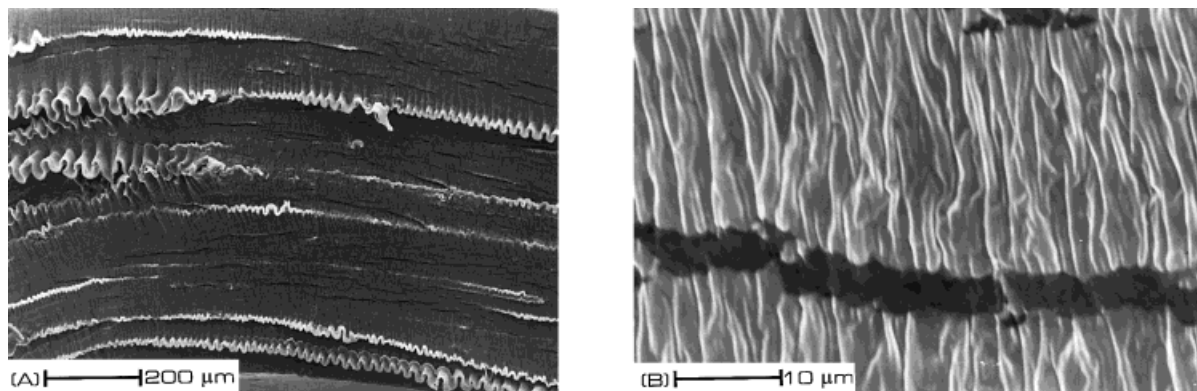


**Figure 11.** SEM pictures depicting the fracture surface topography of a DDEN-T specimen of ELPP-B.

in astonishing fracture morphology pictures. Figure 10(a) and (b) show a torn multimicrolayer structure across the specimen thickness. The torn layers with sinusoidal wave pattern are oriented parallel to the surface of the specimen and load axis. The authors are not aware of the development of this texture elsewhere, except thermoplastic elastomers.<sup>20</sup> According to the author,<sup>20</sup> the undulation on the fracture surface in TPEs is due to an alternating crack growth between the crack flanks. In our opinion, some morphology rearrangement yielding plastic deformation should also be involved. This affects the elastic recovery after fracture producing these undulated patterns.

This structure dominates all of the fracture landscape, as Figure 11(b) demonstrates. In the same picture, dark stripes are visible, deployed parallel to the elastic layers. Focussing on them at a higher magnification helped identify these darker stripes as crazes, which are generated due to the difference in the moduli between the elastic layers and the stiffer crystalline matrix domains surrounding them.

## SUMMARY

Based on the thermal, mechanical, and fracture analysis of elastomeric PP (ELPP) polymers presented above, the following conclusions can be drawn: (1) the thermal behavior of ELPP is controlled on their molecular and supermolecular (crystalline) structure. (2) The essential work of fracture can be adopted for the toughness characterization of ELPP types, either under mode I or mode III conditions. The selection of the suitable experimental approach, appears to be dependent

on the relation between tensile and tearing characteristics. (3) The specific essential work of fracture increased, whereas the nonessential or plastic work decreased with decreasing crystallinity of the ELPP. This tendency can be attributed to the synergistic effect of the molecular entanglement in the amorphous phase and the physical network structure, in which crystalline aggregates form “knots.”

## ACKNOWLEDGMENTS

Part of this work was performed in a project supported by the German Science Foundation (DFG Ka 1202/4-1). The authors wish to thank the PCD Polymere GmbH for providing the materials investigated and release of this article; the samples were mostly prepared in a project supported by the Austrian Forschungsförderungsfonds für die gewerbliche Wirtschaft (FFF) under Proj. No. 3/11688.

## REFERENCES

1. G. H. Llinas, S.-H. Dong, D. T. Mallin, M. D. Rausch, Y.-G. Lin, H. H. Winter, and J. C. W. Chien, *Macromolecules*, **25**, 1242 (1992).
2. W. J. Gauthier, in *Polypropylene: An A-Z Reference*, J. Karger-Kocsis, Ed., Chapman & Hall/Kluwer Academic, London, 1998, p. 178.
3. R. Mülhaupt, in *Polypropylene: An A-Z Reference*, J. Karger-Kocsis, Ed., Chapman & Hall/Kluwer Academic, London, 1998, p. 454.
4. M. Gahleitner, H. Ledwinka, N. Hafner, H. Heineemann, and W. Neißl, Proc. of Special Polyolefins '96, Houston, TX, 1996, p. 251.
5. W. J. Gauthier and S. Collins, *Macromol.Symp.*, **98**, 223 (1995).



6. M. H. Masproch, O. O. Santana, J. Grando, D. Ferrer, and A. B. Martinez, *Polym. Bull.*, **39**, 249 (1997).
7. M. Farina, *Macromol. Symp.*, **95**, 489 (1995).
8. A. G. Atkins and Y.-W. Mai, *Elastic and Plastic Fracture*, Ellis Horwood, Chichester, 1988.
9. S. Hashemi, *Polym. Eng. Sci.*, **37**, 1912 (1997).
10. J. Karger-Kocsis, T. Czigány, and E. J. Moskala, *Polymer*, **38**, 4587 (1997).
11. T. Vhu-Khanh, *Theor. Appl. Fract. Mech.*, **21**, 83 (1994).
12. K. B. Broberg, *J. Mech. Phys. Solids*, **23**, 215 (1975).
13. J. Karger-Kocsis, T. Czigány, and E. J. Moskala, *Polymer*, **39**, 3939 (1998).
14. A. Gray, Testing protocol for the essential work of fracture,ESIS TC-4 group, 1993.
15. A. N. Gent and J. Jeong, *J. Mater. Sci.*, **21**, 355 (1986).
16. J. Karger-Kocsis and T. Czigány, *Polymer*, **37**, 2433 (1996).
17. J. Karger-Kocsis and E. J. Moskala, *Polym. Bull.*, **39**, 503 (1997).
18. D. E. Mouzakis, F. Stricker, R. Mülhaupt, and J. Karger-Kocsis, *J. Mater. Sci.*, **33**, 2551 (1998).
19. G. M. Kim, G. H. Michler, M. Gahleitner, and J. Fiebig, *J. Appl. Polym. Sci.*, **60**, 1391 (1996).
20. E. L. Rodriguez, *J. Mater. Sci. Lett.*, **16**, 1994 (1997).